Real Time Infrared Spectroscopic Probe of the Reactions of $Fe(CO)_3$ and $Fe(CO)_4$ with N_2 in the Gas Phase

Jiaqiang Wang, Gregory T. Long,† and Eric Weitz*

Department of Chemistry, Northwestern University, Evanston, Illinois 60208-3113

Received: August 29, 2000; In Final Form: November 1, 2000

Time-resolved infrared absorption spectroscopy has been used to study the gas-phase reactions of $Fe(CO)_3$, $Fe(CO)_3N_2$, and $Fe(CO)_4$ with N_2, where $Fe(CO)_3$ is generated by 308 nm laser photolysis of $Fe(CO)_5$. The heretofore unknown complex $Fe(CO)_3(N_2)_2$ forms by addition of N_2 to $Fe(CO)_3N_2$ with a rate constant of $(5.4 \pm 1.8) \times 10^{-16}$ cc molecule^{-1} s^{-1}. This rate constant is much smaller than is typical for the addition of small ligands to coordinately unsaturated metal carbonyls, and data are consistent with this reaction being activated. The bond dissociation energy (BDE) for the loss of a N_2 ligand from $Fe(CO)_4N_2$ is 17.6 ± 1.8 kcal mol^{-1}. The activation energy for the loss of N_2 from $Fe(CO)_3(N_2)_2$ is 14.1 ± 5.2 kcal mol^{-1}. The kinetics of the system are consistent with a model that involves equilibria between $Fe(CO)_3$, $Fe(CO)_3N_2$, and $Fe(CO)_3(N_2)_2$ as well as reactions of coordinatively unsaturated species with $Fe(CO)_5$. Using this kinetic model, an upper limit for the BDE for the Fe−N_2 bond in $Fe(CO)_3N_2$ has been estimated and the BDE for the Fe−N_2 bond in $Fe(CO)_3(N_2)_2$ has been determined under the assumption that one of the relevant reactions has a minimal activation energy.

I. Introduction

The photochemistry of organometallic compounds is a broad and still relatively unexplored area of research. Photolysis of organometallic complexes can generate coordinatively unsaturated species which find applications in organometallic synthesis, bond activation reactions, and a variety of catalytic processes.[1,2] It has now been convincingly demonstrated that transient infrared spectroscopy can be used to directly obtain information about the structures and reactivities of short-lived coordinatively unsaturated metal carbonyls generated in such photochemical processes.[2−6]

Addition of molecular nitrogen to transition metal centers has long been a topic of interest.[7] The photochemical synthesis of dinitrogen complexes of some metals has been reported.[8−13] These include the monodinitrogen Mo,[13] Ni,[8] W,[11] and Fe[10,12] carbonyls. A bisdinitrogen tungsten carbonyl complex has been generated, and the $Fe(N_2)_5$ complex has been observed in a matrix at 15 K.[14] Coordinatively saturated chromium carbonyls of the type $Cr(CO)_y(N_2)_{6-y}$ with 1−6 dinitrogen ligands (y = 0−5) have also been observed.[9] Though dinitrogen and carbon monoxide are isoelectronic, a number of studies have shown that the differences in their interactions with metal centers are striking.[14,15] These differences exhibit themselves in both bonding interactions and reaction kinetics. For example, a large difference between the addition rates of CO and N_2 ligands to the triplet 16-electron complex, $Cp^*MoCl(PMe_3)_2$, in the liquid phase, has been reported.[15] A recent theoretical investigation highlighted the unique features of bonding in CO and compared it to a variety of other ligands with particular emphasis on the role of σ donation and back-bonding in these interactions.[16]

To better understand the interaction between ligand(s) and metal centers, more knowledge of the structure, bond energies, and the reactivity of the species involved in such processes is required. Basic thermodynamic and kinetic information is also vital to evaluating the viability of proposed reaction schemes and catalytic pathways.[17] However, so far there have been no experimental measurements of bond dissociation energies (BDEs) of iron−dinitrogen complexes that we are aware of. Only the Cr−N_2 BDE in $Cr(CO)_5N_2$ and the Ni−N_2 BDE in $Ni(CO)_3N_2$ have been determined in the liquid phase,[13,8] whereas the Fe−N_2 BDE in $Fe(CO)_4N_2$ and the BDEs for metal−N_2 bonds in $M(CO)_5N_2$ (M = Cr, Mo, and W) have been calculated.[16−18]

The gas phase provides an environment in which fundamental kinetic and mechanistic processes can be studied in the absence of solvent effects. Measurements of the rate constants for $Fe(CO)_3 + N_2$, $Fe(CO)_4 + N_2$, and $Fe(CO)_3N_2 + CO$ were carried out by House and Weitz in this environment.[12] In one of the few other real time kinetic studies of reactions of N_2 with a coordinatively unsaturated species, Ishikawa et al.[11] investigated the gas-phase reaction of $W(CO)_5 + N_2$.

In this paper, we report detailed microscopic kinetic data for the reactions of $Fe(CO)_3$ and $Fe(CO)_4$ with N_2 and the first measurement of the bond dissociation energy of $Fe(CO)_4N_2$. We also have measured the activation energy for the loss of N_2 from the heretofore unknown complex $Fe(CO)_3(N_2)_2$ and provide a determination of the BDE for this complex with the assumption that one of the reactions involved in the kinetics of the system does not have a significant activation energy. A kinetic model for reactions taking place in this system also provides a means to estimate the BDE for $Fe(CO)_3N_2$. The work in this paper is complimented by a parallel theoretical study of Fe and Cr complexes of the form $Fe(CO)_x(N_2)_{5-x}$ and $Cr(CO)_y(N_2)_{6-y}$ (x = 0−4 and y = 0−5). This latter study emphasizes the effect of the N_2 for CO substitution on bonding modalities and BDEs in the resulting complexes.[20]

II. Experimental Section

A detailed description of the time-resolved IR apparatus used in this study is available in refs 3 and 4. A brief description is

* To whom correspondence should be addressed.
† Current address: Department of Chemistry, University of Utah, Salt Lake City, UT.

10.1021/jp003096s CCC: $20.00 © 2001 American Chemical Society
Published on Web 03/27/2001

given here for convenience. The excimer laser photolysis source, operating at 308 nm (XeCl), delivered ~6 mJ/cm^2 at the front window of the sample cell. The infrared diode probe laser was double passed through a 42 cm long 2.5 cm diameter static gas sample cell terminated with CaF_2 windows and was then focused onto the element of a fast InSb detector with a minimum intrinsic response time of ~250 ns. The signal from the InSb detector was amplified and sent to a digital oscilloscope where it was digitized and averaged for 10−30 traces. Experiments were performed to verify that the total cell pressure was high enough to ensure that the bimolecular reactions under study were in the high-pressure limit.[2−4] If higher pressures were desired, then helium was added.

The time-resolved infrared spectra were constructed from waveforms acquired at probe frequencies within the carbonyl stretch region by joining together the amplitude of various waveforms at common delay times. Kinetic information was determined from transient waveforms collected at a particular probe frequency, as a function of the pressure of the reactant of interest. These signals were fit to exponentials using commercial software. Unless otherwise stated, all experiments were performed at a cell temperature of 24 ± 1 °C. Except where otherwise noted, all errors are reported as 2σ from linear regression fits.

The BDE of $Fe(CO)_4N_2$ was measured using static cell fills of 0.10 Torr $Fe(CO)_5$, 25−216 Torr N_2, and ~10 Torr CO. The kinetics of $Fe(CO)_3N_2$ were studied using cell fills of 0.020−0.250 Torr $Fe(CO)_5$, 30−320 Torr N_2, and enough He to bring the total pressure up to at least 100 Torr. The decay of $Fe(CO)_3(N_2)_2$ was studied using cell fills of ~0.05 Torr $Fe(CO)_5$, 30−310 Torr N_2, and enough He to bring the total pressure up to at least 100 Torr.

$Fe(CO)_5$ of >99% purity was obtained from Aldrich Chemical and put through a series of freeze−pump−thaw cycles before use. The following gases were obtained from Matheson at the stated purities and used as received: N_2, 99.9995%; CO, 99.9%; He, 99.999%.

III. Results and Discussion

A. Spectra. The 308 nm photolysis of $Fe(CO)_5$ produces $Fe(CO)_3$ as the only observable photoproduct.[21−24] The following reactions are plausible for association processes that could take place after the generation of $Fe(CO)_3$ in the presence of $Fe(CO)_5$ and N_2:

$$Fe(CO)_3 + N_2 \xrightarrow{k_1} Fe(CO)_3N_2 \quad (1)$$

$$Fe(CO)_3N_2 + N_2 \xrightarrow{k_2} Fe(CO)_3(N_2)_2 \quad (2)$$

$$Fe(CO)_3N_2 + Fe(CO)_5 \xrightarrow{k_3} Fe_2(CO)_8N_2 \quad (3)$$

$$Fe(CO)_3 + Fe(CO)_5 \xrightarrow{k_4} Fe_2(CO)_8 \quad (4)$$

The time-resolved infrared spectra produced by 308 nm photolysis of a mixture of $Fe(CO)_5$ and N_2 is shown in Figure 1A. It has been reported that $Fe(CO)_3N_2$ has an absorption starting in the low 1960 cm^{-1} region and extending into the mid 1970 cm^{-1} region.[12] The data in Figure 1A show an absorbing species with two peaks in this region, with the strongest of these absorptions at 1966 cm^{-1}. The data shown is for a time period after the initially generated $Fe(CO)_3$ has reacted with N_2. As expected for two absorptions that belong to the same species, they have a common time dependence for reactions with N_2.

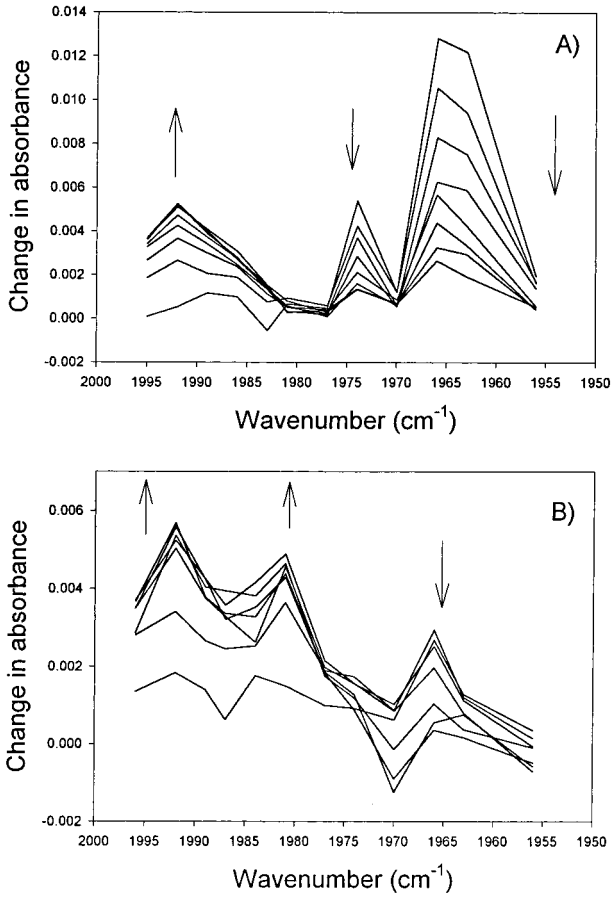

Figure 1. (A) Time-resolved infrared spectra generated upon 308 nm photolysis of a mixture of 100 mTorr $Fe(CO)_5$ and 50 Torr N_2. The spectra cover a total time range from 20 to 160 μs, with each successive trace incremented by 20 μs from the first trace which is 20 μs after the laser pulse. (B) Time-resolved infrared spectra generated upon 308 nm photolysis of a mixture of 100 mTorr $Fe(CO)_5$, 10 Torr CO, and 50 Torr N_2. The spectra cover a total time range from 3 to 24 μs, with each successive trace incremented by 3 μs from the first trace which is 3 μs after the laser pulse. The direction of growth or decay is indicated by the arrows. See text for assignments.

Poliakoff[25] reported two absorptions of matrix-isolated $Fe(CO)_3N_2$ at 1954 and 1948 cm^{-1}. In going from the condensed phase to the gas phase, CO stretching absorptions typically exhibit a shift toward higher frequency of between 10 and 20 cm^{-1}. Thus, the wavelengths reported by Poliakoff for $Fe(CO)_3N_2$ in a matrix are consistent with prior reports[12] of gas-phase absorptions for $Fe(CO)_3N_2$ and are also consistent with those observed in these experiments at 1973 and 1966 cm^{-1}. Therefore, the absorptions in Figure 1A, at 1973 and 1966 cm^{-1}, are assigned to $Fe(CO)_3N_2$.

The data in Figure 2 demonstrate that the decay of $Fe(CO)_3N_2$, as monitored at 1966 cm^{-1}, matches the rise of a new species with an absorption at 1992 cm^{-1}. This latter absorption is also apparent in Figure 1A. In addition, an absorption is observed at 2026 cm^{-1} that has the same rise rate as the 1992 cm^{-1} absorption. However, because the region around the 2026 cm^{-1} absorption is convoluted with very strong absorptions of $Fe(CO)_5$,[24] it was difficult to definitively determine the peak of this absorption band. It should also be noted that the 1992 cm^{-1} band appears to have a shoulder to its low-frequency side. Though this feature is subtle, it is observed in multiple spectra taken under different conditions. The dip at short Δt in the lower

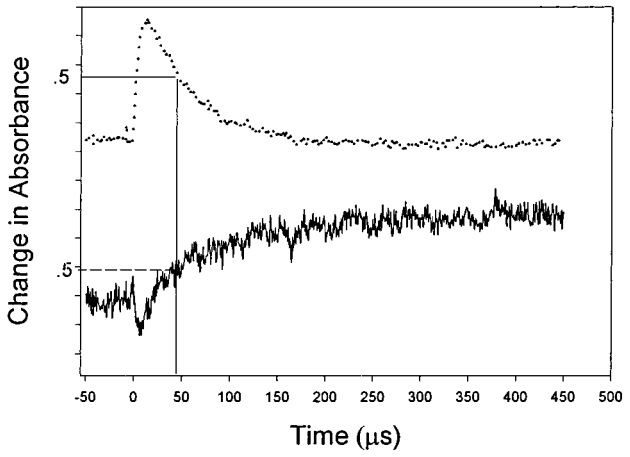

Figure 2. Comparison of the transient absorption signals acquired at 1966 (upper trace) and 1992 cm^{-1} (lower trace) after photolyzing 50 mTorr $Fe(CO)_5$ in the presence of 100 Torr N_2. The traces show the decay of $Fe(CO)_3N_2$ at 1966 cm^{-1} and the growth of $Fe(CO)_3(N_2)_2$ at 1992 cm^{-1}. Horizontal lines are drawn to the 50% points on the two traces.

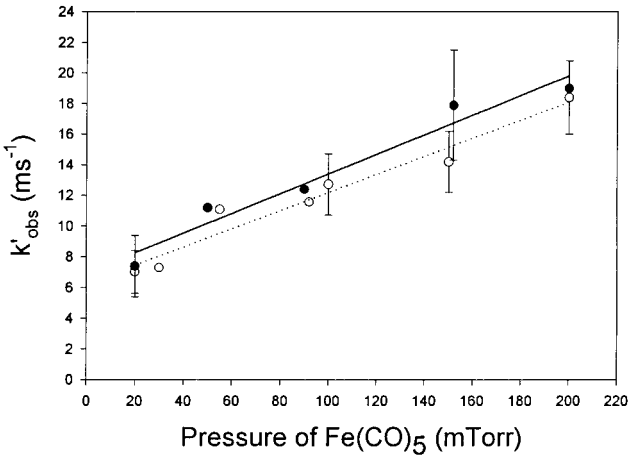

Figure 3. Plot of k'_{obs} (see eq 14) for the decay of $Fe(CO)_3N_2$ vs $Fe(CO)_5$ pressure in the presence of 320 Torr N_2. Experimental results at 280 K (●) and 304 K (○). The solid (280 K) and dotted (304 K) lines are calculated from eq 14.

trace in Figure 2 (the 1992 cm^{-1} absorption) is likely due to photolytic depletion of $Fe(CO)_5$, because the probe frequency overlaps the tail of the $Fe(CO)_5$ absorption band in this region.

Because the absorptions of $Fe_2(CO)_8$ are known and the absorption at 1992 cm^{-1} is only observed when N_2 is added to the photolysis cell, from the above scheme, the species that absorbs at 1992 cm^{-1} could only be the result of reactions 2 and/or 3, i.e., it could be $Fe(CO)_3(N_2)_2$ and/or $Fe_2(CO)_8N_2$.

The rate constants for reactions 2 and 3 are $(5.4 \pm 1.8) \times 10^{-16}$ and $(4.3 \pm 2.2) \times 10^{-13}$ cc molecule^{-1} s^{-1} (obtained from fitting data for the dependence of the rate of decay of $Fe(CO)_3N_2$, k'_{obs}, on N_2 and $Fe(CO)_5$ pressure, see section III.B.2). It can be calculated from these rate constants that at 0.1 Torr $Fe(CO)_5$ and 50 Torr N_2 nearly half of the reaction products are polynuclear species. The plot of the decay of $Fe(CO)_3N_2$, monitored at 1966 cm^{-1}, as a function of $Fe(CO)_5$ pressure is shown in Figure 3. This process is due to reaction 3. The interpretation of the data in Figure 3 is discussed in section II.B.2. The significant intercepts in this plot (>5 ms^{-1}) are an indicator that there are reactions competing with reaction 3. Though in principle CO that is generated by the photolysis of $Fe(CO)_5$ could react with $Fe(CO)_3N_2$, the amount of CO produced from the photolysis of $Fe(CO)_5$ is not enough to yield an intercept of the observed magnitude. Additionally, as the pressure of $Fe(CO)_5$ approaches zero, the pressure of photolytically produced CO also approaches zero, and thus, addition of CO to $Fe(CO)_3N_2$ should not contribute to the intercept. Also, both the rise and decay of the 1992 cm^{-1} absorption are N_2 dependent. Only reaction 2 fits these criteria. Therefore, reaction 2 occurs in this system and the new species formed from this reaction is assigned as the disubstituted complex, $Fe(CO)_3(N_2)_2$. In further support of this assignment, within experimental error, at constant N_2 pressure, the amplitude of the ratio of the absorptions due to $Fe(CO)_3(N_2)$ and $Fe(CO)_3(N_2)_2$ scale linearly with $Fe(CO)_5$ pressure over the range from 50 to 200 mTorr. This would be expected because reaction 3, which competes with reaction 2, becomes relatively more important as the $Fe(CO)_5$ pressure is increased.

TABLE 1: Absorptions of Various $Fe(CO)_x(N_2)_y$ Species in the Gas Phase

molecule	frequency (cm^{-1})
$Fe(CO)_4$	2000, 1984[21]
$Fe(CO)_3N_2$	1973, 1966 [this work]
$Fe(CO)_5$	2013, 2034[24]
$Fe(CO)_4N_2$	1992, 1984 [this work]
$Fe(CO)_3(N_2)_2$	1986 (sh), 1992, 2026 [this work]

Figure 1B shows that when CO is added to the $Fe(CO)_5/N_2$ mixture in the photolysis cell the shape of the resulting transient spectrum changes significantly. The rate of formation of the absorption at 1992 cm^{-1} increases with added CO, and the absorption in the 1984 cm^{-1} region becomes much sharper. Cooper and Poliakoff [10] reported absorptions for $Fe(CO)_4N_2$ at 2235, 2083.3, 2006.8, 1981.6, and 1971.7 cm^{-1} in a high-density polyethylene film. When the expected shift from the condensed phase to the gas phase was considered, the corresponding CO stretching absorptions of gas-phase $Fe(CO)_4N_2$ would be expected at ~2096, ~2020, ~1995, and ~1985 cm^{-1}. The two lower frequency absorptions expected for $Fe(CO)_4N_2$ agree very well with the peaks that grow in the presence of both N_2 and CO. There are obvious explanations as to why the two higher frequency CO stretching absorptions seen by Cooper and Poliakoff were not observed in this work. The absorption at 2020 cm^{-1} will overlap strongly with an $Fe(CO)_5$ absorption in this region,[24] and the absorption at 2096 cm^{-1} is out of the range of diode laser used in these experiments. Consistent with the assignment of these absorptions to $Fe(CO)_4N_2$, House and Weitz[12] assigned absorptions they observed at 1992 and 1984 cm^{-1}, under similar reaction conditions, to $Fe(CO)_4(N_2)$.

The absorptions observed for the species of relevance to this study are tabulated in Table 1. As indicated in the above discussion and in Table 1, $Fe(CO)_4N_2$ and $Fe(CO)_3(N_2)_2$ both have absorptions at 1992 cm^{-1}. Reference 20 discusses the factors that lead to shifts in the frequencies of the CO stretching absorptions in complexes of this type as N_2 is substituted for CO.

As discussed in ref 20, the low frequency shoulder on the 1992 cm^{-1} absorption band of $Fe(CO)_3(N_2)_2$ that was alluded to earlier in this section is relevant to the assignment of the geometry of the lowest energy isomer of $Fe(CO)_3(N_2)_2$ and therefore warrants additional attention. This shoulder is in the same region as an absorption of $Fe(CO)_4N_2$, and $Fe(CO)_4N_2$ could form even in the absence of added CO as a result of the addition of photolytically generated CO to either $Fe(CO)_3$ (with subsequent addition of N_2) or to $Fe(CO)_3N_2$. However, the position of the shoulder is somewhat shifted from the peak of the $Fe(CO)_4N_2$ absorption and the shoulder is present even at very high nitrogen pressure. Thus, we assign this shoulder as

due to an absorption of $Fe(CO)_3(N_2)_2$. However, we consider this assignment tentative in light of the nature of the data that lead to the assignment. Nevertheless, it should be noted that our assignment of the absorptions at 1992 and 2026 cm^{-1} to $Fe(CO)_3(N_2)_2$ are independent of the nature of the absorbing species that generates the shoulder observed on the 1992 cm^{-1} absorption.

B. Kinetics. *1. Reactions in the Presence of CO: The Bond Dissociation Energy of $Fe(CO)_4N_2$.* When sufficient CO is added to the photolysis mixture, $Fe(CO)_4N_2$ is the dominant stable product (see Figure 1B). $Fe(CO)_4N_2$ can be formed by two parallel pathways: the reaction of $Fe(CO)_3N_2$ with CO and $Fe(CO)_4$ with N_2. At a pressure 10 Torr of CO and 50 Torr of N_2, the dominant reaction pathway for formation of $Fe(CO)_4N_2$ involves addition of CO to $Fe(CO)_3(N_2)$.[12]

Because $Fe(CO)_4N_2$ can be produced via these reactions, it should be possible to determine its BDE using a procedure that has been successfully applied to other substituted metal carbonyls in the gas phase.[26] BDEs can be determined from appropriate kinetic measurements based on the mechanism indicated below. The mechanism and the relevant kinetic development have been described in detail previously.[2,26,27] This mechanism is applicable for dissociative loss of a ligand. Dissociative loss is expected for weakly bound ligands, especially when "slippage" of an already bound ligand, which could result in opening up a coordination site, is not possible. Without ligand slippage, a reaction involving an associative ligand substitution process would require a six-coordinate intermediate that is greater than an 18-electron species, which would be expected to involve a significant activation energy.[7] The association reactions (6−8) relevant to the determination of the $Fe(CO)_4-N_2$ BDE are shown below:

$$Fe(CO)_4N_2 \xrightarrow{k_d} Fe(CO)_4 + N_2 \quad (5)$$

$$Fe(CO)_4 + N_2 \xrightarrow{k_6} Fe(CO)_4N_2 \quad (6)$$

$$Fe(CO)_4 + CO \xrightarrow{k_7} Fe(CO)_5 \quad (7)$$

$$Fe(CO)_4 + Fe(CO)_5 \xrightarrow{k_8} Fe_2(CO)_9 \quad (8)$$

A closed form solution for the kinetics described by reactions 5−8 can be obtained using the steady-state approximation for $Fe(CO)_4$. With this treatment, the observed rate for the loss of $Fe(CO)_4N_2$ (and rate for reforming $Fe(CO)_5$) is[26]

$$k_{obs} = \frac{k_d(k_7[CO] + k_8[Fe(CO)_5])}{k_6[N_2] + k_7[CO] + k_8[Fe(CO)_5]} \quad (9)$$

Figure 4 shows that $Fe(CO)_5$ is regenerated in this system and that the rate of regeneration matches the rate of decay of $Fe(CO)_4N_2$. By varying the N_2 and CO pressures, k_d can be calculated. From eq 9, it is clear that if the pressure of N_2 and/or CO is high enough $k_8[Fe(CO)_5]$ will be negligible relative to at least one of the other terms in the denominator. When the term $k_8[Fe(CO)_5]$ is neglected, eq 9 can be rewritten to obtain an explicit expression for k_d, the rate constant for dissociative loss of N_2. Neglecting the term $k_8[Fe(CO)_5]$ yields

$$k_d = \left(1 + \frac{k_6[N_2]}{k_7[CO]}\right)k_{obs} \quad (10)$$

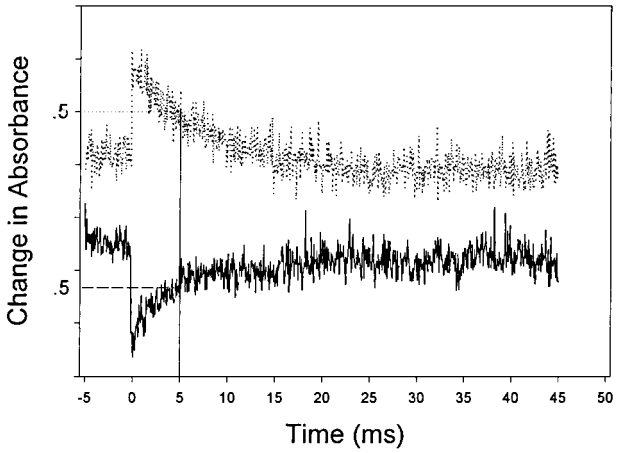

Figure 4. Comparison of the transient absorption signals acquired at 1992 cm^{-1} (upper trace) and at 2044 cm^{-1} (lower trace) following the 308 nm photolysis of 100 mTorr $Fe(CO)_5$ in the presence of 100 Torr N_2 and 10 Torr CO. The traces show the decay of $Fe(CO)_4N_2$ at 1992 cm^{-1} and the recovery of $Fe(CO)_5$ at 2044 cm^{-1}. Horizontal lines are drawn to the 50% points on the two traces.

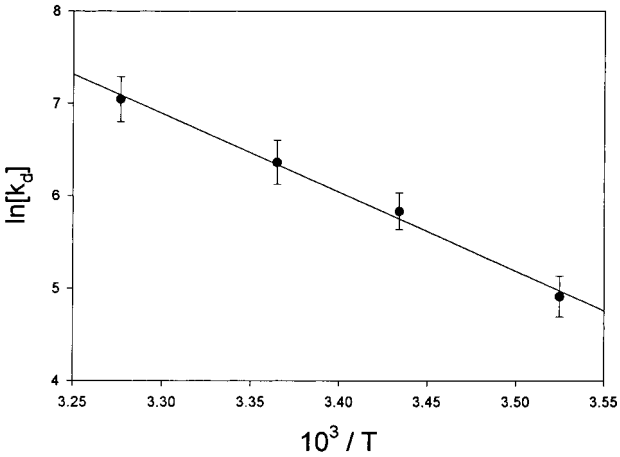

Figure 5. Arrhenius plot for the loss of N_2 from $Fe(CO)_4N_2$. The units for k_d are s^{-1}.

Under these circumstances, k_{obs} should depend on the $[N_2]/[CO]$ ratio rather than the individual N_2 and CO pressures. For example, for 100 mTorr $Fe(CO)_5$, $k_{obs} = 0.124 \pm 0.004$ ms^{-1} with 10 Torr CO and 100 Torr N_2, which agrees well with $k_{obs} = 0.119 \pm 0.008$ ms^{-1} obtained for a mixture containing 20 Torr CO and 200 Torr N_2.

To determine the temperature dependence of k_d from the temperature dependence of k_{obs}, the temperature dependence of k_6 and k_7 must be known or determined. Within experimental error, over the temperature range from 279 to 304 K, there was no variation in k_6, which was measured by probing the rate of growth of $Fe(CO)_4N_2$ at 1980 cm^{-1}. Thus, within the error limits, the addition of N_2 to $Fe(CO)_4$ is unactivated. This observation is consistent with the general trend that has been observed for the addition of small ligands to coordinatively unsaturated metal carbonyls.[28,29] For example, it has previously been reported that, within error limits, k_7, the rate constant for the reaction of $Fe(CO)_4$ with CO, is temperature-independent from 283 to 328 K.[29] Present results, obtained for k_7 from 279 to 304 K, support the conclusion that, within the error limits, k_7 is unactivated.

A plot of k_d vs $10^3/T$ is shown in Figure 5. This Arrhenius plot yields an activation energy of 17.0 ± 1.7 kcal mol^{-1} with

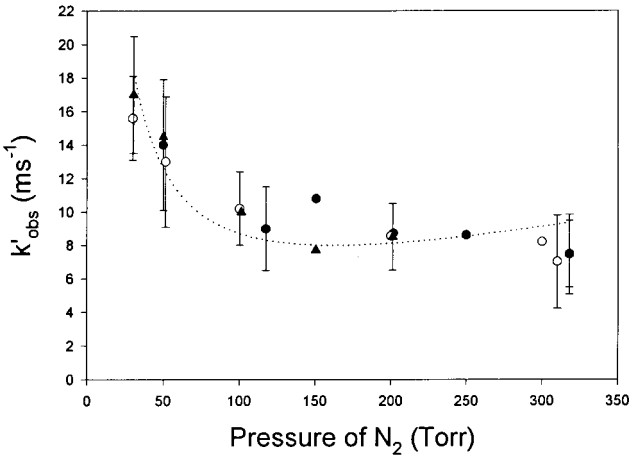

Figure 6. Plot of k'_{obs} (see eq 14) for the decay of $Fe(CO)_3N_2$ vs N_2 pressure in the presence of 0.02 Torr $Fe(CO)_5$. Experimental results at 275 (●), 283 (○), and 297 K (▲). The dashed line is a fit of the 297 K data to the form of eq 14.

an intercept, ln *A*, of 35.1 ± 3.0. When the relevant ligand association processes are unactivated, as is the case for $Fe(CO)_4N_2$, the activation energy for loss of a ligand can be directly related to the bond enthalpy.[26] Using this procedure, the enthalpy change for reaction 5

$$Fe(CO)_4N_2 \xrightarrow{k_d} Fe(CO)_4 + N_2 \qquad (5)$$

is 17.6 ± 1.8 kcal mol^{-1} at 297 K.

Radius et al.[16] computed the bond dissociation enthalpies for C_{3v} and C_{2v} $Fe(CO)_4-N_2$ at 298 K and obtained values of 18.1 and 19.0 kcal mol^{-1}, respectively. These values are in good agreement with the value of 17.6 ± 1.8 kcal mol^{-1} obtained in the present study for 297 K. More recently, Weitz and co-workers[20] calculated the bond dissociation enthapies for this system to be 18.1 kcal mol^{-1} for the lowest energy C_{2v} isomer of $Fe(CO)_4-N_2$, at 298 K, which also agrees well with the present experimental determination of the BDE.

For $Fe(CO)_5$, the first bond dissociation enthalpy of 41 ± 2 kcal mol^{-1} [19] is approximately twice as large as the BDE for the loss of N_2 from $Fe(CO)_4N_2$. Walsh et al.[13] determined the BDE of $Cr(CO)_5(N_2)$ to be 19 ± 1 kcal mol^{-1} using photoacoustic calorimetry in heptane. This value is also close to one-half that of the Cr−CO bond BDE in $Cr(CO)_6$, which has a value of 37 ± 2 kcal mol^{-1}.[19] Clearly, in these systems, replacing a CO by an N_2 leads to a less stable compound. Issues involved in the change in stability of such complexes as a result of the substitution of dinitrogen ligands for CO are treated in more detail in ref 20.

2. Reactions in the Absence of Added CO. The reaction kinetics of $Fe(CO)_3N_2$ were probed using its 1966 cm^{-1} absorption. As would be anticipated, the rate of decay of $Fe(CO)_3N_2$ increased with increasing $Fe(CO)_5$ pressure (Figure 3). However, surprisingly, the rate of decay of $Fe(CO)_3N_2$ *decreased with increasing N_2 pressure* up to at least 150 Torr (Figure 6). Within experimental error, the rates for the loss of $Fe(CO)_3N_2$ at 1966 cm^{-1}, as a function of N_2 pressure, were the same as the rates of rise of $Fe(CO)_3(N_2)_2$ at 1992 cm^{-1}. The *decreasing* decay rate of $Fe(CO)_3N_2$ with *increasing N_2 pressure* suggests that $Fe(CO)_3N_2$ is very unstable and readily loses N_2. Thus, an equilibrium between $Fe(CO)_3N_2$ and $Fe(CO)_3$ must be included in the description of the kinetics of this system.

It has been reported that some other $M(CO)_x(N_2)$ complexes, such as $Ni(CO)_3N_2$,[8] $CpV(CO)_3(N_2)$,[30] and chromium complexes of the form $Cr(CO)_{6-x}(N_2)_x$[9] readily lose N_2. For $CpV(CO)_3(N_2)$[30] an equilibrium was observed and the rate of loss of $CpV(CO)_3(N_2)$ *decreased as the N_2 pressure was increased*. For the $Fe(CO)_3N_2$ system, because there is an equilibrium between $Fe(CO)_3N_2$ and $Fe(CO)_3$, $Fe(CO)_3$ is present as a steady-state intermediate. Thus, the reaction of $Fe(CO)_3 + Fe(CO)_5$ must also be included in a global description of the kinetics of the system.[21] Additionally, prior results on analogous systems and data from this study indicate that $Fe(CO)_3L$ compounds (where L is a ligand) can react with $Fe(CO)_5$.[31] Therefore, the reaction of $Fe(CO)_3N_2$ and $Fe(CO)_5$ is included in the following kinetic scheme which can be used to explain the above observations:

$$Fe(CO)_3 + N_2 \xrightarrow{k_1} Fe(CO)_3N_2 \qquad (1)$$

$$Fe(CO)_3N_2 \xrightarrow{k_{-1}} Fe(CO)_3 + N_2 \qquad (11)$$

$$Fe(CO)_3N_2 + N_2 \xrightarrow{k_2} Fe(CO)_3(N_2)_2 \qquad (2)$$

$$Fe(CO)_3(N_2)_2 \xrightarrow{k_{-2}} Fe(CO)_3N_2 + N_2 \qquad (12)$$

$$Fe(CO)_3N_2 + Fe(CO)_5 \xrightarrow{k_3} Fe_2(CO)_8N_2 \qquad (3)$$

$$Fe(CO)_3 + Fe(CO)_5 \xrightarrow{k_4} Fe_2(CO)_8 \qquad (4)$$

Using a treatment similar to that in refs 32 and 33, the rate of decay of $Fe(CO)_3N_2$, indicated as k'_{obs}, can be obtained as follows:

$$k'_{obs} = \frac{N}{M} \qquad (13)$$

where

$$N = k_{-2}(k_3[Fe(CO)_5] + k_1[N_2] + k_{-1} + k_4[Fe(CO)_5]) + k_1[N_2](k_2[N_2] + k_3[Fe(CO)_5]) + k_4[Fe(CO)_5](k_2[N_2] + k_{-1} + k_3[Fe(CO)_5])$$

and

$$M = k_{-1} + k_1[N_2] + k_2[N_2] + k_3[Fe(CO)_5] + k_4[Fe(CO)_5] + k_{-2}$$

The magnitudes of k_1 and k_4 are known,[12,21] and from the values that are determined (vide infra) for k_{-1}, k_{-2}, k_2, and k_3, it is clear that when $[N_2]$ is ≥ 10 Torr and $[Fe(CO)_5]$ is ≤ 0.2 Torr $k_1[N_2]$ will be the dominant term in the denominator and eq 13 can be simplified to give

$$k'_{obs} = k_{-2} + k_2[N_2] + k_3[Fe(CO)_5] + k_4[Fe(CO)_5]k_{-1}/k_1[N_2] \qquad (14)$$

To evaluate eq 14, k_{-2}, the rate constant for dissociation of $Fe(CO)_3(N_2)_2$, must be determined. This was done by monitoring the decay of $Fe(CO)_3(N_2)_2$ at 1992 cm^{-1} as a function of N_2 pressure and employing the following development.

On a long time scale (>100 ms), the steady-state approximation can be applied to $Fe(CO)_3N_2$, because this species decays to close to the baseline on a much shorter time scale (<0.5 ms). The relevant reactions involved in the formation and decay of $Fe(CO)_3(N_2)_2$ are

$$Fe(CO)_3(N_2)_2 \xrightarrow{k_{-2}} Fe(CO)_3N_2 + N_2 \quad (12)$$

$$Fe(CO)_3N_2 + N_2 \xrightarrow{k_2} Fe(CO)_3(N_2)_2 \quad (2)$$

$$Fe(CO)_3N_2 + Fe(CO)_5 \xrightarrow{k_3} Fe_2(CO)_8N_2 \quad (3)$$

With the application of the steady-state approximation to $Fe(CO)_3N_2$, a closed form expression for the rate of decay of $Fe(CO)_3(N_2)_2$ (indicated as k''_{obs}) can be obtained from reactions 12, 2, and 3:

$$k''_{obs} = \frac{k_{-2}k_3[Fe(CO)_5]}{k_2[N_2] + k_3[Fe(CO)_5]} \quad (15)$$

A plot of $1/k''_{obs}$ vs N_2 pressure is shown in Figure 7. From this plot and eq 15, the following can be determined:

$$\text{intercept} = \frac{1}{k_{-2}} \quad (16)$$

and

$$\text{slope} = \frac{k_2}{k_{-2}k_3[Fe(CO)_5]} \quad (17)$$

Using this treatment, k_{-2} was determined to be 177 ± 54 s^{-1} at room temperature (24 °C), and using this value for k_{-2} and eq 17, $k_3 = (800 \pm 300)k_2$.

k_{-2} is sufficiently small compared with the other terms in eq 14 that it can be neglected. k_3 and k_2 are related by the relationship $k_3 = (800 \pm 300)k_2$, and k_1 and k_4 are known.[12,21] k_{-1} and k_2 were obtained using eq 14 and the following procedure. k_{-1} and k_2 were varied, and the values that produced the best agreement between the value of k'_{obs} calculated using eq 14 and experimental data for k'_{obs} as a function of N_2 pressure were selected. The term involving k_{-1} is dominant at low pressures of N_2, and the term involving k_2 becomes increasingly important as the N_2 pressure increases. This fitting procedure gave the following results:

$k_{-1} = (1.0 \pm 0.4) \times 10^6$ s^{-1} and $k_2 = (5.4 \pm 1.8) \times 10^{-16}$ cc molecule^{-1} s^{-1} at room temperature (24 °C). From this value for k_2 and the relationship between k_2 and k_3 indicated above, k_3 is $(4.3 \pm 2.2) \times 10^{-13}$ cc molecule^{-1}s^{-1}. As a further check on the validity of the values of these rate constants, they were used to calculate the dependence of k'_{obs} (eq 14) on $Fe(CO)_5$ pressure. These calculated values, which are shown in Figure 3, agreed within experimental error with the measured values for k'_{obs}.

It is interesting to note that the rate constant for the reaction of $Fe(CO)_3N_2 + Fe(CO)_5$ to give $Fe_2(CO)_8N_2$, k_3, which has been estimated as $(4.3 \pm 2.2) \times 10^{-13}$ cc molecule^{-1}s^{-1}, is virtually identical to the rate constant measured for the reaction of $Fe(CO)_4 + Fe(CO)_5$ of $\sim 5 \times 10^{-13}$ cc molecule^{-1}s^{-1}.[21] Thus, whether the L in $Fe(CO)_3L$ is CO or N_2 does not have a significant effect on the reactive behavior of $Fe(CO)_3L$ with $Fe(CO)_5$. As previously discussed, this is very different than what has been observed for the reaction of coordinatively unsaturated iron carbonyls with CO and N_2 themselves. However, it is certainly plausible that the properties of N_2 would not have a significant effect on a reaction when the N_2 is incorporated in another reacting moiety (as it is in $Fe(CO)_3N_2$) relative to when the reaction involves N_2 itself as the adduct.

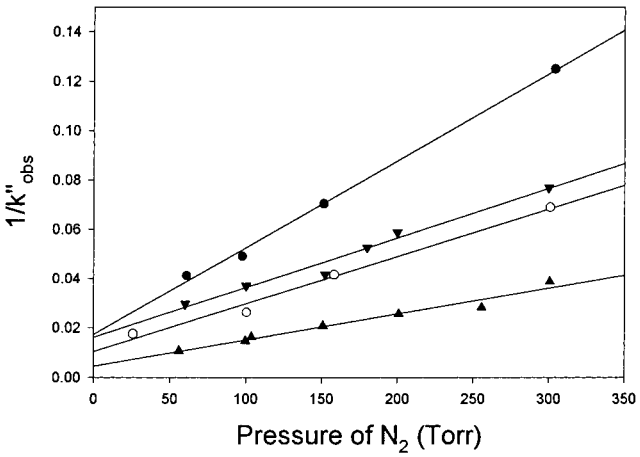

Figure 7. Plot of $1/k''_{obs}$ (at 1992 cm^{-1}) vs N_2 pressure at 283 (●), 291 (▼), 297 (○), and 304 K(▲). k''_{obs} has units of s^{-1}.

As the N_2 pressure is increased, the equilibria described by eqs 1, 2, 11, and 12 will shift toward the nitrogen adducts. Initially, the rate of decay of $Fe(CO)_3(N_2)$ decreases because of the N_2 dependent term in the denominator of the fourth term in eq 14. However, at sufficiently high N_2 pressure, the second term in eq 14, $k_2[N_2]$, will become larger than the fourth term, $k_4[Fe(CO)_5]k_{-1}/k_1[N_2]$. When this occurs, the rate of decay of $Fe(CO)_3(N_2)$ (k'_{obs}) will increase with nitrogen pressure. For example, at 297 K, it is calculated that k'_{obs} will increase from 8.1 to 9.4 ms^{-1} when the N_2 pressure is increased from 200 to 320 Torr. However, this magnitude change is within our experimental error, and no difference in rates was experimentally observed for such a pressure change.

Equations 1−4, 11, and 12 are the simplest set of equations that have reproduced all of the experimental data including the very unusual *decrease* in the rate of decay of $Fe(CO)_3N_2$ with increasing nitrogen pressure. Elimination of any of these equations results in a model that no longer reproduces all of the experimental data.

The rate constant for reaction 4, k_4, can be determined in the absence of both added CO and N_2 by monitoring the formation of $Fe_2(CO)_8$ at 2048 cm^{-1}.[21] From this measurement, k_4 is $2.91 \pm 0.29 \times 10^{-10}$ and $1.89 \pm 0.25 \times 10^{-10}$ cm^3 molecule^{-1} s^{-1} at 275 and 305 K, respectively. When these two values are taken in conjunction with the previous results measured at room temperature of $2.93 \pm 0.46 \times 10^{-10}$ cm^3 molecule^{-1} s^{-1},[21] an activation energy E_a for k_4 of -0.92 ± 0.99 kcal mol^{-1} can be calculated. Because this activation energy is within the experimental error of zero, we conclude that this reaction has a very small activation energy which could be zero or negative. A small negative activation energy would not be inconsistent with the mechanism that has been proposed for formation of polynuclear complexes in this system.[2,21]

Small negative activation energies have been previously reported for the reaction of C_2H_3 with HCl[35] and the reaction of $C(CH_3)_3$ with HI. These negative activation energies have been ascribed to the reaction being rate limited by formation of a complex.[36] It has previously been postulated that reactions that lead to polynuclear complexes with bridging bonds must proceed via complex formation and the rearrangement necessary to form these bridging bonds occurs after the rate-limiting complexation step.[2,21] A small negative activation energy for k_4 is plausible for such a mechanism.[34]

C. Bond Dissociation Energy for $Fe(CO)_3N_2$ and $Fe(CO)_3(N_2)_2$. The rate of decay of $Fe(CO)_3(N_2)_2$ (k''_{obs}) as a function of pressure is shown in Figure 7. As seen in eq 16, the rate for

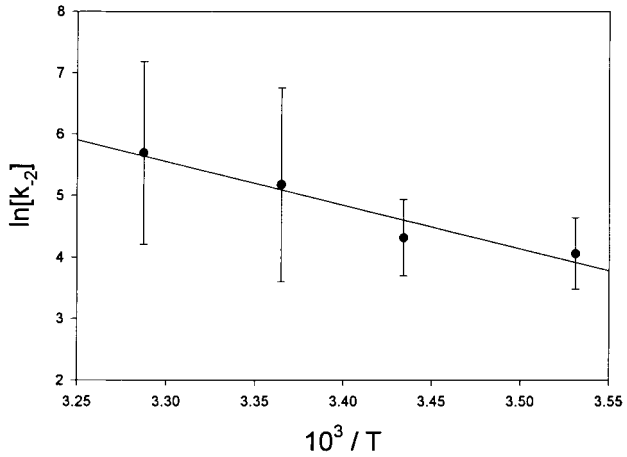

Figure 8. Arrhenius plot for the loss of N_2 from $Fe(CO)_3(N_2)_2$. The units for k_{-2}, are s^{-1}.

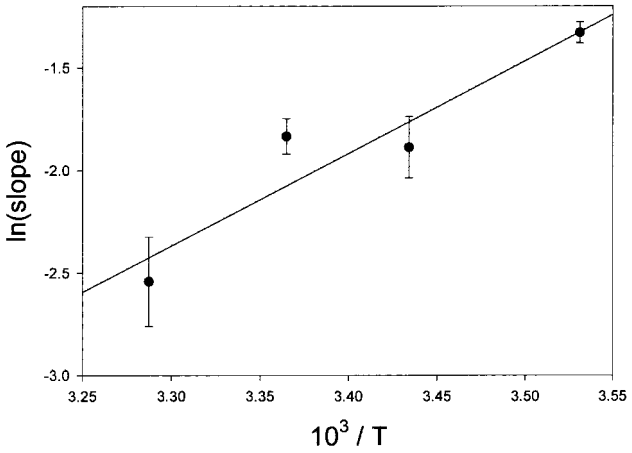

Figure 9. Plot of the ln (slope) versus $10^3/T$, where the slope being plotted is obtained from eq 17 for a standard state of SATP.

the loss of N_2 from $Fe(CO)_3(N_2)_2$, k_{-2}, is directly related to the inverse of the intercept in this plot. An Arrhenius plot of k_{-2} as a function of $10^3/T$ is shown in Figure 8. This plot gives $E_a = 14.1 \pm 5.2$ kcal mol^{-1} and ln $A = 28.9 \pm 9.0$.

As was previously indicated, the rate constant for the reaction of $Fe(CO)_3N_2 + Fe(CO)_5$ to give $Fe_2(CO)_8N_2$, which was estimated as $(4.3 \pm 2.2) \times 10^{-13}$ cc molecule^1 s^{-1}, is virtually identical to the magnitude of the rate constant measured for the reaction of $Fe(CO)_4 + Fe(CO)_5$ of $\sim 5 \times 10^{-13}$ cc molecule^{-1} s^{-1}. The fact that this latter reaction has been observed in a matrix at 15 K effectively precludes a significant positive activation energy.[37] As such, we assume that reaction 3 is unactivated. With this assumption, the temperature dependence of the slope in eq 17 can be directly related to the temperature dependence of k_2/k_{-2} and, thus, to the equilibrium constant for the equilibrium between $Fe(CO)_3(N_2) + N_2$ and $Fe(CO)_3(N_2)_2$. Data for the temperature dependence of the slope in eq 17, using a standard state of 298 K and one bar, plotted vs $10^3/T$, is shown in Figure 9. These data give an enthalpy change for this reaction of -9.0 ± 4.6 kcal/mol. Though a negative activation energy for reaction 3 is not precluded, it would be expected to be small. A plausible value for a negative activation energy for k_3 would still give an enthalpy that fell within the quoted error limits. The enthalpy change of -9.0 ± 4.6 kcal/mol and the measured activation energy of 14.1 ± 5.2 kcal mol^{-1} for the loss of N_2 from $Fe(CO)_3(N_2)_2$ can be used in the context of a propagation of errors treatment to deduce an activation energy of 5.7 ± 3.6 kcal/mol for the reaction of N_2 with $Fe(CO)_3N_2$ (eq 2).

Equation 14 contains a term involving k_{-1}/k_1. Thus, in principle this equation could be used to obtain the bond enthalpy for $Fe(CO)_3N_2$. However, the experimental error in the individual temperature-dependent rate constants leads to large errors in k_1/k_{-1}, and additionally, approximations are required to determine the rate constants necessary to evaluate the temperature dependence of k_1/k_{-1}, including the relationship $k_3 = (800 \pm 300)k_2$. Clearly, if k_3 is not activated and k_2 is activated, there cannot be a temperature *independent* expression relating the two rate constants. However, the error limits on the data are large enough that the data does not allow us to determine the actual temperature dependence of the relationship between k_3 and k_2. Thus, an alternative approach was used to obtain an approximate value for the BDE for the $Fe-N_2$ bond in $Fe(CO)_3N_2$. A value for k_{-1} of $(1.0 \pm 0.4) \times 10^6$ s^{-1} has been determined from fitting the relationship in eq 14 to the experimental data. The preexponential for loss of N_2 from $Fe(CO)_4N_2$ has been determined as 1.6×10^{15} with error limits that correspond to approximately 1 order of magnitude. If a similar preexponential is assumed for k_{-1}, the activation energy for loss of N_2 from $Fe(CO)_3N_2$ is between $\sim 11-14$ kcal/mol. Although an activation energy for the forward reaction would lead to a smaller bond enthalpy, there is no experimental evidence for an activation energy for a *spin allowed* addition of a small ligand to an unsaturated metal carbonyl. Even if this process were activated, because the rate constant for reaction 1 is within a factor of ~ 20 of gas kinetic, the activation energy would have to be less than 2 kcal/mol. Additionally, within the operative error limits the conversion between activation energy and bond enthalpy is insignificant. Thus, we can conclude that the $Fe-N_2$ bond in $Fe(CO)_3N_2$ is weak and, from the data obtained in this work, ~ 14 kcal/mol is an effective upper limit for this BDE. A smaller preexponential than what is discussed above is possible and perhaps even likely based on the fitting of the temperature dependence of the data to eq 14. However, a smaller preexponential would lead to a smaller BDE which would be within the upper limit for the BDE that is quoted.

D. Comparison of Rate Constants for the addition of N_2 and CO to $Fe(CO)_3N_2$. A comparison between rates of reaction of CO and N_2 is particularly intriguing. CO and N_2 are isoelectronic ligands. Interestingly, there is a dramatic difference between the rate constant for the reaction of $Fe(CO)_3N_2$ with CO relative to the rate constant for the reaction of $Fe(CO)_3N_2$ with N_2, with the former being more than 1500 times larger than the latter. Both of these reactions involve the addition of a ligand to a 16 e$^-$ triplet species to produce an 18 e$^-$ singlet product. Interestingly, as reported by Keogh and Poli,[15] there is a similar difference (on the order of 3 orders of magnitude) in the rates of addition of these ligands to a triplet 16 e$^-$ organometallic molecule, $Cp^*MoCl(PMe_3)_2$. Reactions of $Fe(CO)_3L$ with L (L = CO, C_2H_2, and C_2F_4) are generally faster than reactions of $Fe(CO)_4$ with L. $Fe(CO)_3N_2$ follows this trend for CO but not for N_2. Additionally, the reported reactions of $W(CO)_4N_2$ with N_2 are slower than for $W(CO)_5$ with N_2.[11]

It is interesting to speculate as to the source of this difference in rate constants for these two ligands. Reactions of iron species that go from a triplet tetracoordinate to a singlet pentacoordinate complex for *both* ligands are expected to involve a curve crossing. Factors that can influence curve crossing probabilities have been discussed in ref 2. Less overlap between the orbitals of the iron centered complex and N_2 bonding orbitals relative to overlap with CO bonding orbitals could change the position where the singlet and triplet curves cross. Consistent with this hypothesis, a recent theoretical study of the nitrogen substituted

iron carbonyl complexes concludes there is less orbital overlap for N_2 relative to CO. Within the context of the model presented in ref 2 differences in overlap of bonding orbitals could then lead to a barrier to reaction, or a change in the height of a barrier, and thus a smaller rate constant for reaction of N_2 than for corresponding reactions of CO.

However, independent of the exact value of the activation energy for the reaction of N_2 with $Fe(CO)_3N_2$, when judged in the context of other data on the magnitude of rate constants for the association reaction of small ligands with coordinatively unsaturated metal carbonyls,[27] this reaction has a very small rate constant. This is consistent with an earlier report that there was no clear evidence for a reaction when the $Fe(CO)_3N_2 + N_2$ system was initially studied at low N_2 pressure and on a relatively short time scale.[12] A similar observation of an apparent lack of a reaction has been reported for $Fe(CO)_3H_2 + H_2$.[38] It is interesting to speculate whether further study of this latter system would also lead to the conclusion that this latter addition process has a small rate constant and is activated.

IV. Conclusions

$Fe(CO)_3N_2$ reacts with N_2 to form $Fe(CO)_3(N_2)_2$, a complex that has not been previously observed. Interestingly, this reaction may be an exception with respect to other addition reactions of small ligands to coordinatively unsaturated metal carbonyls, which are typically unactivated, in that the data are consistent with this process having an activation energy of 5.7 ± 3.6 kcal/mol. The bond dissociation energy for the loss of a N_2 ligand from $Fe(CO)_4N_2$ is 17.6 ± 1.8 kcal mol^{-1} at 297 K. A global kinetic model, that includes equilibria between $Fe(CO)_3(N_2)_2$ and $Fe(CO)_3N_2 + N_2$ and between $Fe(CO)_3N_2$ and $Fe(CO)_3 + N_2$ can explain all of the experimental observations for these species and can be used to deduce a number of kinetic parameters for this system. The activation energy for the loss of N_2 from $Fe(CO)_3(N_2)_2$ is 14.1 ± 5.2 kcal mol^{-1}. The BDE for $Fe(CO)_3(N_2)_2$ was determined to be 9.0 ± 4.6 kcal/mol at 298 K, with the assumption that the reaction of $Fe(CO)_3N_2 + Fe(CO)_5$ does not have a significant activation energy. $Fe(CO)_3N_2$ is a weakly bound complex with a BDE that is no larger than $\sim$14 kcal/mol.

Acknowledgment. We acknowledge support of this work by the National Science Foundation under Grant NSF 97-34891. We thank one of the referees for pointing out the expected relationship between the amplitude of the $Fe(CO)_3(N_2)$ and $Fe(CO)_3(N_2)_2$ signals as a function of $Fe(CO)_5$ pressure.

References and Notes

(1) Leadbeater, N. L. *Coord. Chem. Rev.* **1999**, *188*, 35.
(2) Weitz, E. *J. Phys. Chem.* **1994**, *98*, 11256.
(3) Weitz, E. *J. Phys. Chem.* **1987**, *91*, 3945.
(4) Poliakoff, M.; Weitz, E. *Adv. Organomet. Chem.* **1986**, *25*, 277.
(5) George, M. W.; Poliakoff, M.; Turner, J. J. *Analyst* **1994**, *119*, 551.
(6) George, M. W.; Turner, J. J. *Coord. Chem. Rev.* **1998**, *177*, 201.
(7) Collman, J. P.; Hegedus, L. S.; Norton, J. R. *Principles and Applications of Organotransition Metal Chemistry*; University Science Books: Mill Valley, CA, 1987.
(8) Turner, J. J.; Simpson, M. B.; Poliakoff, M.; Maier, W. B., II *J. Am. Chem. Soc.* **1983**, *105*, 3898.
(9) Turner, J. J.; Simpson, M. B.; Poliakoff, M.; Maier, W. B., II; Graham, M. A. *Inorg. Chem.* **1983**, *22*, 911. DeVore, T. C. *Inorg. Chem.* **1976**, *15*, 1315.
(10) Cooper, A.; Poliakoff, M. *Chem. Phys. Lett.* **1993**, *212*, 611.
(11) Ishikawa, Y.; Hackett, P. A.; Rayner, D. M. *J. Phys. Chem.* **1989**, *93*, 652.
(12) House, P. G.; Weitz, E. *Chem. Phys. Lett.* **1997**, *266*, 239.
(13) Walsh, E. F.; Popov, V. K.; George, M. W.; Poliakoff, M. *J. Phys. Chem.* **1995**, *99*, 12016. Burdett, J. K.; Downs, A. J.; Gaskill, G. P.; Graham, M. A.; Turner, J. J.; Turner, R. F. *Inorg. Chem.* **1978**, *17*, 523.
(14) Doeff, M. M.; Parker, S. F.; Barret, P. H.; Pearson, R. G. *Inorg. Chem.* **1984**, *23*, 4108.
(15) Keogh, D. W.; Poli, R. *J. Am. Chem. Soc.* **1997**, *119*, 2516.
(16) Radius, U.; Bickelhaupt, F. M.; Ehlers, A. W.; Goldberg, N.; Hoffmann, R. *Inorg. Chem.* **1998**, *37*, 1080.
(17) Dapprich, S.; Pidun, U.; Ehlers, A. W.; Frenking, G. *Chem. Phys. Lett.* **1995**, *242*, 521.
(18) Wullen, C. V. *J. Chem. Phys.* **1996**, *105*, 5485.
(19) Lewis, E. K.; Golden, D. M.; Smith, G. P. *J. Am. Chem. Soc.* **1984**, *106*, 3905.
(20) Cedeno, D. L.; Weitz, E.; Berces, A. *J. Phys. Chem. A* **2001**, *105*, 3773.
(21) Ryther, R. J.; Weitz, E. *J. Phys. Chem.* **1991**, *95*, 9841.
(22) Rayner, D. M.; Ishikawa, Y.-I.; Brown, C. E.; Hackett, P. A. *Laser Chemistry of Organometallics*; Chaiken, J., Ed.; ACS Symposium Series, No. 530; American Chemical Society: Washington, DC, 1993; p 96.
(23) Long, G. T.; Weitz, E. *J. Am. Chem. Soc.* **2000**, *117*, 12810.
(24) Ryther, R. J.; Weitz, E. *J. Phys. Chem.* **1992**, *96*, 2561.
(25) Poliakoff, M. *J. Chem. Soc., Dalton Trans.* **1974**, 210.
(26) Bogdan, P. L.; Wells, J. R.; Weitz, E. *J. Am. Chem. Soc.* **1991**, *113*, 1294.
(27) House, P. G.; Weitz, E. *J. Phys. Chem. A* **1997**, *101*, 2988.
(28) Wells, J. R.; House, P. G.; Weitz, E. *J. Phys. Chem.* **1994**, *98*, 8343.
(29) Seder, T. A.; Ouderkirk, A. J.; Weitz, E. *J. Chem. Phys.* **1986**, *85*, 1977.
(30) George, M. W.; Haward, M. T.; Hamley, P. A.; Hughes, C.; Johnson, F. P. A.; Popov, V. K.; Poliakoff, M. *J. Am. Chem. Soc.* **1993**, *115*, 2286.
(31) Long, G. T.; Wang, W.; Weitz, E. *J. Am. Chem. Soc.* **1995**, *117*, 12810.
(32) Buxton, G. V.; Salmon, G. A.; Wang, J. *Phys. Chem. Chem. Phys.* **1999**, *1*, 3589.
(33) Buxton, G. V.; Bydder, M.; Salmon, G. A. *Phys. Chem. Chem. Phys.* **1999**, *1*, 269.
(34) Smith, I. W. M Kinetics and dynamics of elementary gas reactions. *Butterworths Monographs in Chemistry and Chemical Engineering*; Butterworths: Boston, MA, 1980.
(35) Krueger, H.; Weitz, E. *J. Chem. Phys.* **1988**, *88*, 1608.
(36) Richard, P. D.; Ryther, R. J.; Weitz, E. *J. Phys. Chem.* **1990**, *94*, 3663.
(37) Fletcher, S. C.; Poliakoff, M.; Turner, J. J. *Inorg. Chem.* **1986**, 25, 3597.
(38) Hayes, D. M.; Weitz, E. *J. Phys. Chem.* **1991**, *95*, 2723.